Effects of hole-boring and relativistic transparency on particle acceleration in overdense plasma irradiated by short multi-PW laser pulses

Masahiro Yano

Graduate School of Engineering, Osaka University

1. introduction

Recently the power of femtosecond laser pulses has exceeded the petawatt level and is continuously increasing [1]. Intensities over 10^{23} W/cm^2 ($a_0 \sim 300$, where a_0 is the normalized laser field [2,3]) at the laser focus have already been reached [4]. Several upcoming projects [5-9] make possible laser intensities exceeding $I \sim 10^{24}$ W/cm^2 or $a_0 \sim 10^3$. That would be a qualitative step forward in high field physics, because the parameter ma_0/M, where M is the proton mass, becomes of the order of unity. Such powerful laser pulses can directly accelerate heavy particles up to relativistic energies. Moreover, the effect of relativistic transparency theoretically allows laser pulse propagation through even solid density plasmas. The latter, along with the generation of energetic particles, has been of particular interest.

Specific to the interaction of powerful laser pulses and overdense plasmas is the relativistic effects in the plasma. A multi-PW laser pulse has a normalized vector potential $a_0 = eE/mc\omega$ [where E is the amplitude of the laser field and ω is the laser pulse frequency] far exceeding unity. Therefore, the group velocity of a laser pulse in plasma $v_G = \sqrt{1 - 4\pi e^2 N_e/m\omega^2 a_0}$ [2,3] remains positive for electron densities which are a_0 times higher than the critical density $N_{cr} = m\omega^2/4\pi e^2$. For Ti-Sph laser pulses and the laser intensity $I = 10^{24}$ W/cm^2, the maximal density is $N_{emax} = 2 \times 10^{24}$ cm^{-3}. However, the equation for the group velocity is correct only for the electron figure-eight motion which could be restricted by the transverse components of the plasma field. Additionally, the hole-boring process [10-20] can also allow high intensity laser pulses to propagate through a spatially semi-infinite overdense plasma. Due to the laser ponderomotive force, $F_p = -\frac{1}{4}\frac{mc^2}{\gamma}\nabla a_0^2$ [2,3] electrons are pushed at the front of laser pulses while the main body of the pulses propagates in a much lower density plasma. Again, such processes as pulse filamentation and other instabilities can drastically diminish this force and finally stop the hole-boring process. How far powerful laser pulses can propagate in a spatially semi-infinite overdense plasma with different density and the domains of validity of such a process have yet to be fully understood.

Another important feature of the interaction of ultra-high intensity laser pulses with plasma is the possibility of direct acceleration of heavy ions by laser pulses. The general solution of particle motion in the plane wave gives [2,3,21-30]:

$$\gamma = \sqrt{(M/m)^2 + p_X^2 + p_Y^2}; \ \gamma - p_X = A; \ p_Y = a_0\cos(\omega t - \frac{\omega x}{c}),$$

where M is the ion mass, A is a constant and p is normalized by mc, the particle momentum. If the ion is initially at rest, $A = M/m$ and $p_X = mp_Y^2/2M$. For $a_0 > M/m$ the energy of ion becomes relativistic even in a vacuum. In a relativistically transparent plasma, this effect may occur as a self-injection process for ions at the front of a laser pulse.

In this letter, we investigate numerically the dynamics of ultra-intense laser pulses and the generation of energetic particles in spatially semi-infinite, overdense hydrogen plasma. Multidimensional PIC simulations including fully relativistic motions for electrons and ions as well as the classical radiation friction force are performed with high spatial $\lambda/200$ in 2D and maximal $\lambda/50$ in 3D using the

code FPlaser [31,32] with the moving window technique. Limited spatial resolution for 3D simulations constrains the range of plasma density and plasma length.

2. Simulation Models

Linearly polarized laser pulses with wavelength $\lambda = 1$ μm and duration $\tau = 10$ fs propagate in the -x (longitudinal) direction from the right to left in a pre-ionized semi-infinite plasma. The laser pulse intensity is varied from 10^{23} to 10^{24} W/cm^2, corresponding to a_0 from $\sim 10^2$ to 10^3. The pulse intensities $10^{23} - 10^{24}$ W/cm^2 at the laser focus correspond to energies from ~ 0.75 kJ to ~ 7.5 kJ and powers of ~ 75 to ~ 750 PW. Laser intensities exceeding $I = 10^{22}$ W/cm^2 have already been achieved [4] and the maximum laser intensity is approaching I=10^{24} W/cm^2 as reported in [5-9], which makes this range of laser intensities interesting for investigation. The initial conditions for the transverse components of the fields are taken as the well-known solution of the para-axial equations [31,32] with the waist w_0=5 μm and corresponding Rayleigh length ~75 μm. In simulations, the size of the moving window is (100 μm)×(100 μm)×(110 μm) to resolve high plasma frequency. The density of the uniform plasma is a parameter ranging from $N_e = 2N_{cr}$ to $100N_{cr}$. Such plasma can be produced in a mixture of high Z gases with hydrogen or in exploding wires [33,34]. However, here we consider pure hydrogen plasma to minimize the number of physical processes. The linear density ramp in the front of the plasma has a length $L = 10$ μm. Absorbing boundary conditions are used in the code [31,32].

3. Results and Discussions

As a result of the simulations, we found that the laser pulses have a finite penetration depth, which depends on the plasma density and initial laser pulse intensity. Typical results are presented in Fig. 1 and Fig.2. In Fig.1 the dependences of the penetration depth, L_D, for laser pulses with different intensity on the plasma density are shown. The penetration depth is calculated as the distance from

the plasma boundary where the laser pulse vanishes or starts moving backward. Even for double critical density and $a_0 \sim 10^3$ the penetration depth is finite; for I=10^{24} W/cm^2 $L_D \sim 300$ μm even though $N_e/N_{cr}a_0$ remains far less than unity. For N_e=$100N_{cr}$ the propagating laser pulse scatters from the boundary. The processes limiting the propagation length can be seen in Fig. 2 where the laser field is given at the stopping point. For lower density, the main reason is the filamentation instability [2,3] as seen in Fig 2a,b, along with the Raman scattering decreasing the pulse intensity. This underlines the role of the hole-boring process in the propagation of laser pulses. Filamented laser pulses cannot form a proper channel for guiding and plasma electrons cannot acquire the energy necessary for the relativistic transparency. With density increase, the transverse plasma field does not allow the 8-figure motion of electrons in the laser field and, as a result, the laser pulse does not penetrate in plasma essentially even though the plasma is still theoretically relativistically transparent. One can see strong scattered light from the plasma surface. With decreasing laser intensity all of the above effects occur earlier and, therefore, L_D becomes smaller.
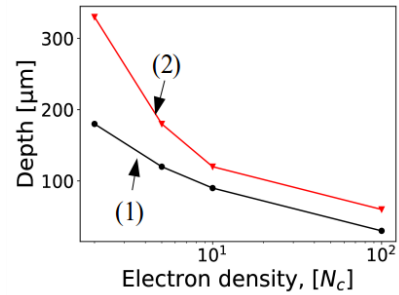

Fig.1 Plot of penetration length for intensities (1) $I = 10^{23}$ W/cm^2, and (2) $I = 10^{24}$ W/cm^2. The penetration length is shorter for higher electron density and lower laser intensity.
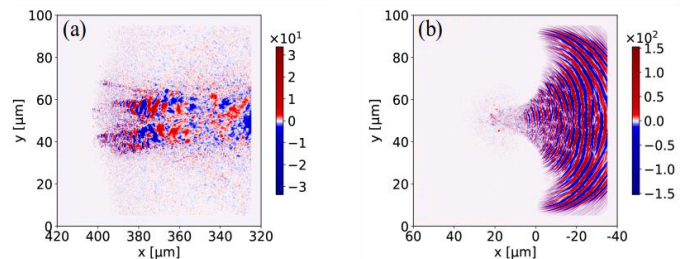
Fig.2 xy cross-section of a laser pulse at the moment when the pulse propagation stops for (a) initial plasma density 2 N_{cr}, intensity $I = 10^{24}$ W/cm^2, the time t=1300fs, (b) initial plasma density 100N_{cr}, intensity $I = 10^{24}$ W/cm^2, the time t=200fs.

During the laser pulse propagation a plasma cavity having a lower density than the surrounding plasma forms in the pulse wake as seen in Fig.3. This is the result of electron evacuation from the laser axis and further ion Coulomb explosion. Therefore, most of the ions acquire large transverse momenta. The cavity shape is dominated by the dynamics of energetic electrons. In Fig.4 a,b the effect of the radiation friction force is illustrated by the shape of cavities with and without it. One can see that the radiation friction force stabilizes the cavity shape. Since the electron density in the cavity is low, the electron acceleration occurs in an underdense plasma driven by the wake field. The results of electron acceleration can be seen in Fig.5a,b for different intensities. As expected, higher energy electrons appear in low, N_e=2N_{cr}, plasma. The maximum electron energy decreases with increasing density reflecting the shortening of the efficient acceleration length in the wake field. The maximum energy increases as a_0 for lower density and increases more slowly at higher density.
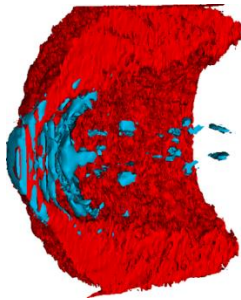

Fig.3 3D plot of a laser pulse and ion density where z > 15 um for initial plasma density 5N_{cr}, intensity $I = 10^{24}$ W/cm^2, and the time t=300fs. Red shows ions. Blue shows a laser pulse. The laser pulse propagates from upper right to lower left.
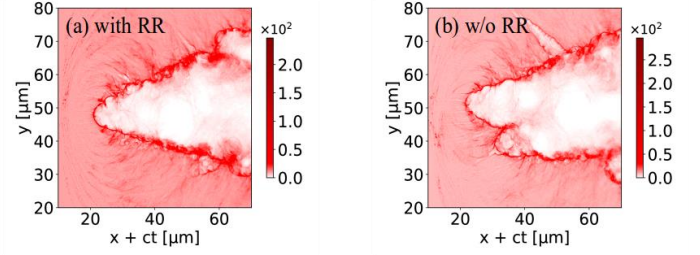

Fig.4 xy cross-section of ion density at the moment when the pulse propagation stops for the initial plasma density 10N_{cr}, intensity $I = 10^{24}$ W/cm^2, the time t=300fs, (a) with radiation reaction force and (b) without radiation reaction force.
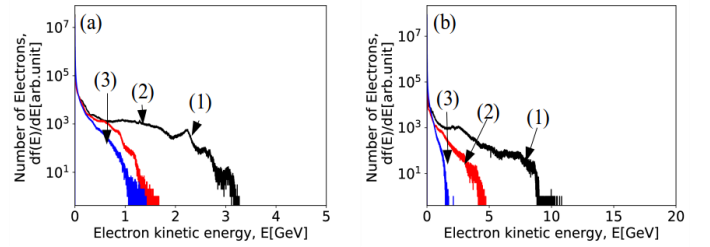

Fig.5 Electron energy spectrum for (a) intensity $I = 10^{23}$ W/cm^2, (b) intensity $I = 10^{24}$ W/cm^2. Lines (1), (2), and (3) indicate the case for initial densities of 2N_{cr}, 5N_{cr}, and 10N_{cr}, respectively.

The results for ion acceleration presented in Fig. 6a,b, show a completely different picture from the case of electron acceleration. The ion energy distribution function at the lower laser intensity, I=10^{23} W/cm^2, is shown in Fig.6a. An increase of plasma density results in slower phase velocity of the plasma wake wave. Since background ions are initially accelerated behind the laser pulse due to the Coulomb explosion, efficient injection of these ions into the plasma wake wave can occur when their velocities match the plasma wake phase velocity. At N_e=10N_{cr} the maximal energy is near 1 GeV. At low density, the maximal ion energy is rather low of the order of 100 MeV. For plasma with density N_e=100N_{cr}, the maximum ion energy is also low. The process of ion acceleration drastically changes for I=10^{24} W/cm^2 where direct ion acceleration becomes more dominant. For lower

plasma density, $N_e = 2N_{cr}$, the direct ion acceleration by the laser pulse serves as an injector of ions into the acceleration phase of the first plasma wave bucket at the front of the laser pulse. Then, a part of such injected ions is accelerated up to 20 GeV. These ions were positioned at the front of the laser pulses in our numerical simulations. With increasing density the direct ion acceleration becomes less efficient for injection as compared to the Coulomb explosion and, therefore, the maximum energy rapidly goes down. The radiation friction force does not affect this mechanism of ion injection and acceleration.
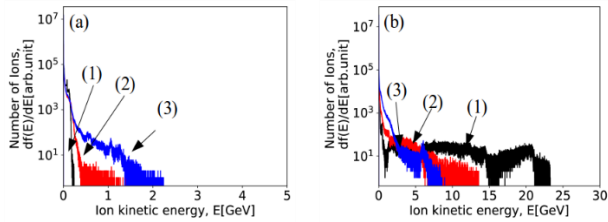

Fig.6 Ion energy spectrum for (a) intensity $I = 10^{23}$ W/cm², (b) intensity $I = 10^{24}$ W/cm². Lines (1), (2), and (3) indicate the case for initial densities of $2N_{cr}$, $5N_{cr}$, and $10N_{cr}$, respectively.

4. Comclusion

In conclusion, we have observed a novel effect of ion acceleration by multi-PW laser pulses in relativistically underdense spatially semi-infinite plasma via fully relativistic PIC simulations including electron and ion motion along with the radiation damping. This acceleration occurs in plasmas with electron densities around 2-10 critical density due to the direct proton acceleration by laser pulses with $a_0 \sim 10^3$ resulting in proton injection into the acceleration phase of the plasma wave at the front of the laser pulses. Protons with energies up to 20 GeV have been observed for 10 fs laser pulses with intensity $I = 10^{24}$ W/cm² irradiating overdense plasma with $N_e = 2N_{cr}$. Such a plasma can be produced by a mixture of a high Z gas and hydrogen. The proton energy rapidly decreases with increasing plasma density. For lower laser intensity the effect vanishes since direct proton acceleration becomes impossible. The behavior of plasma electrons does not show any essential difference from the conventional physical picture and recent experiments with lower laser intensities: energetic electrons form a broad Maxwell-like distribution with an effective temperature proportional to a_0.

Limitation of the laser pulse propagation in a theoretically relativistically transparent spatially semi-infinite plasma has been observed over a wide range of laser intensities and plasma densities. Laser pulse filamentation, backward Raman scattering, and the transverse plasma field break the transparency condition $N_e/N_{cr}a_0 < 1$.

References

[1] C. Danson, D. Hillier, and N. Hopps, D. Neely, High Power Laser Sci. Vol. 3, e3, 14 pages (2015).

[2] E. Esarey and P. Sprangle, IEEE Trans. Plasma Sci. 24, No. 2, 252 (1996); E. Esarey, C. B. Schroeder, and W. P. Leemans, Rev. Mod. Phys. 81, 1229 (2009).

[3] G. A. Mourou, T. Tajima, and S. V. Bulanov, Rev. Mod. Phys. 78 (2006).

[4] J. Shin, H. T. Kim, S. K. Lee, J. H. Sung, H. W. Lee, J. W. Yoon, C. Jeon, and C. H. Nam, The 7th Advanced Lasers and Photon Sources (ALPS2018) (2018)

[5] C.A. Ur, D. Balabanski, G. Cata-Danil, S. Gales, I. Morjan, O. Tesileanu, D. Ursescu, I. Ursu, and N.V. Zamfir, Nucl. Instrum. Methods Phys. Res. B 355, 198-202 (2015).

[6] N. Miyanaga, H. Azechi, K.A. Tanaka, T. Kanabe, T. Jitsuno, J. Kawanaka1, Y. Fujimoto, R. Kodama, H. Shiraga, K. Knodo et al. J. Phys. IV Fr. 133, 81–87 (2006).

[7] J. K. Crane, G. Tietbohl, P. Arnold, E. S. Bliss, C. Boley, G. Britten, G. Brunton, W. Clark, J. W. Dawson, S. Fochs et al. J. Phys. Conf. Ser. 244, 032003 (2010).

[8] D. Batani, M. Koenig, J. L. Miquel, J. E. Ducret, E. d'Humieres, S Hulin, J. Caron, J. L. Feugeas, Ph. Nicolai, V. Tikhonchuk et al. Phys. Scr. 014016 (2014).

[9] D. N. Maywar, D. N. Maywar, J. H. Kelly, L. J. Waxer, S. F. B. Morse, I. A. Begishev, J. Bromage, C. Dorrer, J. L. Edwards, L. Folnsbee, M. J. Guardalben et al. J. Phys. Conf. Ser. 112, 032007 (2008).

[10] N. Iwata, S. Kojima, Y. Sentoku, M. Hata, and K. Mima, Nat. Commun. 9, 623 (2018)

[11] M. Tabak, J. Hammer, M. E. Glinsky, W. L. Kruer, S. C. Wilks, J. Woodworth, E. M. Campbell, and M. D. Perry, Phys. Plasmas 1, 1626 (1994).

[12] R. Kodama, P. A. Norreys, K. Mima, A. E. Dangor, R. G. Evans, H. Fujita, Y. Kitagawa, K. Krushelnick, T. Miyakoshi, N. Miyanaga et al. Nature 412, 798–802 (2001)

[13] M. C. Levy, S. C. Wilks, M. Tabak, S. B. Libby, and M. G. Baring, Nat. Commun. 5, 4149 (2014).

[14] S. C. Wilks, W. L. Kruer, M. Tabak, and A. B. Langdon, Phys. Rev. Lett. 69, 1383–1386 (1992).

[15] A. Pukhov and J. Meyer-ter-Vehn, Phys. Rev. Lett. 79, 2686–2689 (1997).

[16] Y. Sentoku, W. Kruer, M. Matsuoka, and A. Pukhov, Fusion Sci. Technol. 49, 278–296 (2006).

[17] N. Naumova, T. Schlegel, V. T. Tikhonchuk, C. Labaune, I. V. Sokolov, and G. Mourou, Phys. Rev. Lett. 102, 025002 (2009).

[18] Y. Ping, A. J. Kemp, L. Divol, M. H. Key, P. K. Patel, K. U. Akli, F. N. Beg, S. Chawla, C. D. Chen, and R. R. Freeman, Phys. Rev. Lett. 109, 145006 (2012).

[19] S. M. Weng, M. Murakami, H. Azechi, J. W. Wang, N. Tasoko, M. Chen, Z. M. Sheng, P. Mulser, W. Yu, and B. F. Shen, Phys. Plasmas 21, 012705 (2014).

[20] A. L. Lei, A. Pukhov, R. Kodama, T. Yabuuchi, K. Adumi, K. Endo, R. R. Freeman, H. Habara, Y. Kitagawa, and K. Kondo, Phys. Rev. E 76, 066403 (2007).

[21] A. Yogo, K. Mima N. Iwata, S. Tosaki, A. Morace, Y. Arikawa, S. Fujioka, T. Johzaki, Y. Sentoku, H. Nishimura et al. Sci. Rep. 7, 42451 (2017)

[22] H. Daido, M. Nishiuchi, and A. S. Pirozhkov, Rep. Prog. Phys. 75, 056401 71pp (2012).

[23] S. C. Wilks, A. B. Langdon, T. E. Cowan, M. Roth, M. Singh, S. Hatchett, M. H. Key, D. Pennington, A. MacKinnon, and R. A. Snavely, Phys. Plasmas 8, 542 (2001).

[24] R. A. Snavely, M. H. Key, S. P. Hatchett, T. E. Cowan, M. Roth, T. W. Phillips, M. A. Stoyer, E. A. Henry, T. C. Sangster, M. S. Singh et al. Phys. Rev. Lett. 85, 2945–2948 (2000).

[25] T. Esirkepov, M. Borghesi, S. V. Bulanov, G. Mourou, and T. Tajima, Phys. Rev. Lett. 92, 175003 (2004).

[26] L. Yin, B. J. Albright, K. J. Bowers, D. Jung, J. C. Fernández, and B. M. Hegelich, Phys. Rev. Lett. 107, 045003 (2011).

[27] F. Fiuza, A. Stockem, E. Boella, R. A. Fonseca, and L. O. Silva, Phys. Rev. Lett. 109, 215001 (2012).

[28] D. Haberberger, S. Tochitsky, F. Fiuza, C. Gong, R. A. Fonseca, L. O. Silva, W. B. Mori, and C. Joshi, Nat. Phys. 8, pages 95–99 (2012).

[29] B. M. Hegelich, B. J. Albright, J. Cobble, K. Flippo, S. Letzring, M. Paffett, H. Ruhl, J. Schreiber, R. K. Schulze, and J. C. Fernández, Nature 439, 441–444 (2006).

[30] S. Palaniyappan, C. Huang, D. C. Gautier, C. E. Hamilton, M. A. Santiago, C. Kreuzer, A. B. Sefkow, R. C. Shah, and J. C. Fernández, Nat. Commun. 6, 10170 (2015).

[31] A. Zhidkov, T. Fujii, and K. Nemoto, Phys. Rev. E 78, 036406 (2008)

[32] M. Yano, A. Zhidkov, T. Hosokai, and R. Kodama, Phys. Plasma 25, 103104 (2018)

[33] T. Vijayan and V. K. Rohatgi, IEEE T PLASMA SCI. VOL. PS-13, No. 4 (1985)

[34] N. Iwata, H. Nagatomo, Y. Fukuda, R. Matsui, and Y. Kishimoto, Phys. Plasmas 23, 063115 (2016).